Bioelectrochemistry 140 (2021) 107801

Contents lists available at ScienceDirect

Bioelectrochemistry

journal homepage: www.elsevier.com/locate/bioelechem

DNA electrochemical biosensor for detection of *Alicyclobacillus acidoterrestris* utilizing Hoechst 33258 as indicator

José M.R. Flauzino [a,*], Rafaela C.S. Peres [a], Lívia M. Alves [a], Jussara G. Vieira [b], Júlia G. dos Santos [c], Ana G. Brito-Madurro [a], João M. Madurro [b]

[a] Institute of Biotechnology, Federal University of Uberlandia, Uberlandia, Brazil
[b] Institute of Chemistry, Federal University of Uberlandia, Uberlandia, Brazil
[c] Faculty of Chemistry Engineering, Federal University of Uberlândia, Uberlandia, Brazil

ARTICLE INFO

Article history:
Received 29 November 2020
Received in revised form 10 March 2021
Accepted 14 March 2021
Available online 19 March 2021

Keywords:
Alicyclobacillus acidoterrestris
Reduced graphene oxide
3-hydroxybenzoic acid
Hoechst 33258
Orange juice
Genosensor

ABSTRACT

Alicyclobacillus acidoterrestris is an acidophilic and thermophilic bacterium present in the soil, often associated with the spoilage of acidic juices, such as orange juice. Their spores resist pasteurization and, when reactivated, modify the organoleptic properties of the juice, making it unsuitable for consumption, due mainly to production of guaiacol. Biosensors are detection devices that respond quickly and are easy to handle, with great potential for use in the juice production chain. In this context, this work reports an electrochemical genosensor for detection of *A. acidoterrestris,* based on a graphite electrode modified with electrochemically reduced graphene oxide, a polymer derived from 3-hydroxybenzoic acid and a specific DNA probe sequence complementary with the genomic DNA of *A. acidoterrestris*. Detection of the target was performed by monitoring the oxidation peak of the Hoechst 33258, a common DNA stainer. The genosensor detection limit was 12 ng mL^{-1} and it kept 77% of response after ten weeks, and a test showed that orange juice does not interfere with bacteria lysate detection. This biosensor is the first platform for electrochemical detection of the genomic DNA of *A. acidoterrestris* in the literature, and the first to use Hoechst 33258 as indicator with whole genomic DNA molecules.

1. Introduction

Orange juice is one of the most consumed non-alcoholic drinks in the world, due to its antioxidant and nutritional components [1]. The global orange juice industry generates billions of dollars a year, thus being of major commercial impact in regions with large orange production. Due to its low pH and high solids concentration, bacterial proliferation in concentrated orange juice is difficult, however, when it is reconstituted, the juice becomes a suitable medium for bacterial growth [2].

Alicyclobacillus acidoterrestris is a non-pathogenic bacterium present in soil, coming into contact with the fruit at the time of harvest [3]. Even after washing, bacterial biofilms may remain attached in the orange peel, so the bacteria enters in the juice production chain [4]. Due to the presence of ω-alicyclic fatty acids, *A. acidoterrestris* has an extremely temperature-resistant membrane, resisting pasteurization processes commonly applied to orange juice [5]. The main metabolite of *A. acidoterrestris* is guaiacol, which causes medicinal and antiseptic off-flavors, so its presence in orange juice is not desired [6].

Standard method for detection of *A. acidoterrestris* is plating and cultivation in culture medium [7]. Although it is specific, the growth of bacterial colonies takes an average of 48 h, which is not attractive commercially since the juice industry require rapid processes. In addition, there is the need of appropriate laboratory equipment and qualified personnel to perform the tests. Polymerase chain reaction (PCR) method [8] is also used in certain cases, but require the use of expensive reagents, laboratory environment and qualified personnel. Thus, fast and inexpensive methods are needed for detection of this bacteria in juice samples, for its identification and deactivation, avoiding juice spoilage.

Biosensors are fast, cheap and easy-to-use detection devices that can be used throughout the orange juice production chain [9–11]. DNA biosensors (genosensors) are analytical devices resulting from the integration of a specific DNA probe sequence into a transducer [12,13], which generally recognizes the target molecule by the hybridization of the complementary strands [14]. This recognition can be detected directly, through the oxidation of the nitrogenous bases [15], or indirectly through the use of DNA hybridization indicator molecules [16,17]. The use of electroactive

* Corresponding author.
E-mail address: jmflauzino@ufu.br (J.M.R. Flauzino).

https://doi.org/10.1016/j.bioelechem.2021.107801
1567-5394/

DNA binding molecules offers advantages over direct detection, since the oxidation potential of these molecules is generally lower than the oligonucleotide oxidation potentials and it improves the biossensor sensitivity [18]. In both cases, the reaction involves electron transfer, constituting an electrochemical genosensor, which the transducer converts the biological recognition event into an electrical signal [19].

There is a great variety of electroactive substances with DNA affinity, such as ethidium bromide [20], methylene blue [21], tetramethylbenzidine [22], bisbenzimides [23], metallic compounds [24] and others. The bisbenzimide class is widely used in molecular biology as a nucleic acid dye [25]. The german chemical company Hoechst was a pioneer in the production of such compounds, numbering them according to their discovery. The compounds Hoechst 33258, Hoechst 33342, and Hoechst 34580 are the most used for cell nucleous fluorescence microscopy, having a similar structure in which a functional group varies. Hoechst 33258 binds to the double-stranded DNA small groove, thus having no affinity for the single-strand DNA [26]. Kobayashi and colleagues reported its use for the first time as an electrochemical indicator for DNA hybridization quantification [27], when they found that this indicator has a characteristic oxidation peak around 0.5 V (vs. Ag/AgCl), which is attractive because it is a lower potential than the oxidation of the nitrogenous bases of the DNA and another hybridization indicators. In addition, Hoechst 33258 is less mutagenic and carcinogenic than other double-stranded DNA intercalants [28]. These characteristics make this compound of great interest for the construction of DNA detection devices, as it was used by some later works [29,30], but only for detecting small DNA sequences and in purified samples. Thus, the use of Hoechst 33258 for electrochemical detection of large DNA molecules in real samples has not been studied in the scientific literature.

Electrode surface modification has been used to improve detection and quantification of targets, aiming the development of more sensitive devices [31–35]. Mixtures of compounds have been studied to modify electrodes and improve their properties, especially ones containing carbon derived materials, such as carbon nanotubes and graphene, in combination with polymers [36–39]. Graphene oxide is a low-cost material to be obtained and, when reduced, presents properties such as large surface area and high conductivity [40,41]. The combination of reduced graphene oxide with polymers that have functional groups is a great way to modify the electrode surface, allowing interaction with probe biomolecules by the addition of new functional groups [42]. Among these polymers, poly(3-hydroxybenzoic acid) can be easily deposited on the electrode surface, employing electropolymerization by cyclic voltammetry [43]. Compared to the synthesis of other nanocomposites, this process have advantages as it generates the electroactive material directly on the electrode surface, without the need of harmful chemicals, laborious techniques and in a short time [44].

The aim of this work was to develop an electrochemical genosensor for detection of genomic DNA of *A. acidoterrestris* in orange juice sample. For this, a plataform consisting of a graphite electrode modified with electrochemically reduced graphene oxide and poly(3-hydroxybenzoic acid) was built and characterized. The DNA hybridization process was detected utilizing the Hoechst 33258 molecule, a common DNA stainer utilized in fluorescence microscopy, that has also electrochemical activity.

2. Experimental section

2.1. Chemicals and solutions

All reagents were of analytical grade, without previous purification. Ultra high purity water (18.2 MΩ cm^{-1}, Master System, Gehaka, Brazil) was used for preparation of all solutions, wich were deoxygenated by ultrapure nitrogen bubbling in time proportional to volume (1 min mL^{-1}) before use. Hoechst 33258 (2′-(4-hydroxy phenyl)-5-(4-methyl-1-piperazinyl)-2,5′-bi(1H-benzimidazole) trihydrochloride hydrate), sodium dodecyl sulfate (SDS) and bovine serum albumin (BSA) were purchased from Sigma-Aldrich Chemical, USA. Perchloric acid ($HClO_4$) was purchased from Synth, Brazil. Sodium phosphate buffer (Na_2HPO_4 and NaH_2PO_4, 0.1 mol L^{-1}, Neon, Brazil, pH 7.4) was used as support electrolyte for the electrochemical reduction of graphene oxide and for the electrochemical detections. KCl solution (0.1 mol L^{-1}, Neon, Brazil), containing potassium ferrocyanide/ferricyanide solution ($K_4[Fe(CN)_6]/K_3[Fe(CN)_6].3H_2O$, 5 mmol L^{-1}, Acros Organics, USA), was used as anionic redox probe solution. Tris-EDTA buffer (Tris(hydroxymethyl)amino methane-HCl, 10 mmol L^{-1}, Life Technologies, USA and Ethylenediamine tetraacetic acid, 10 mmol L^{-1}, Vetec, Brazil, pH 8.0) were used to store and dilute the genomic DNA samples. DNA probe oligonucleotide for *A. acidoterresitrs* (ALIC1) and the complementary target (ALIC2) were synthesized by Invitrogen Life Technologies (USA) with the following sequences: 5′-CTGTGTTGATGTTGTTGGCG-3′ and 5′-CGCCAACAACATCAACACAG-3′, respectively. These sequences are from the gyrase subunit B gene of *A. Acidoterrestris* and are specific to this specie (GenBank ID: JF713074.1). Oligonucleotide solutions were prepared in sodium citrate buffer (sodium chloride 0.3 mol L^{-1}, sodium citrate 0.03 mol L^{-1}, Sigma-Aldrich, USA, pH 7.0) and stored at −8 °C. Lyophilized *A. acidoterrestris* culture was purchased from Fundação André Tosello (Brazil).

2.2. Apparatus

Voltammetric studies were conducted in a potentiostat from CH Instruments (USA), model 760C. Three-electrode electrochemical cell was employed for the electrochemical experiments. Graphite disks (99.9995% purity, 6.15 mm of diameter Alfa Aesar, USA) were used as working electrodes. Platinum wire was used as auxiliary electrode and Ag/AgCl (KCl 3.0 mol L^{-1}) as reference electrode. A PerkinElmer spectrophotometer in ATR (Attenuated Total Reflectance) mode was used to evaluate the chemical components of the surface of the electrodes. Surface morphology was evaluated by atomic force microscopy (AFM) in a SPM 9600 microscope (Shimadzu) and by scanning electron microscopy (SEM) in a EVO/MA10 microscope (Zeiss). A BioDrop μLite spectrophotometer was used to evaluate the DNA concentration in the solutions.

2.3. Preparation and characterization of the modified graphite electrode

Graphite electrodes (GE) were polished with alumina slurry (0.3 μm), washed with deionized water and dried in the air. The preconditioning of the electrode was performed in $HClO_4$ solution (0.5 mol L^{-1}) by cyclic voltammetry between 0.0 V and +1.2 V, 50 mV s^{-1}, 4 cycles. Graphene oxide (GO) was produced according to the Hummers method [45] with some modifications, as described in previous studies [42]. Graphene oxide was dispersed in water (1 mg mL^{-1}), sonicated for 20 min and drop-casted onto the graphite electrode (20 μL). After dried, the GO was electrochemically reduced by cyclic voltammetry between 0.0 V and −1.5 V, 10 potential cycles, 50 mV s^{-1}, using sodium phosphate buffer as support electrolyte, obtaining the electrochemically reduced graphene oxide (ERGO) on the surface of the electrode. The electrodes were rinsed with deionized water and dried with ultrapure nitrogen. For the electropolimerization of the 3-hydroxybenzoic acid (3-HBA), cyclic voltammetry was applied (0.0 V and +1.2 V, 10 cycles, 50 mV s^{-1}) in $HClO_4$ solution (0.5 mol L^{-1}) containing 3-HBA (2.5 mmol L^{-1}). After electropoly-

merization, 4 potential cycles were performed only in support electrolyte solution ($HClO_4$, 0.5 mol L^{-1}), aiming the oxidation of residual monomer at the electrode surface and acquisition of the resulting electrochemical profile. The surfaces of the GE, GE/GO, and GE/ERGO were analyzed with attenuated total reflection infrared spectroscopy. Graphite electrode modified with poly(3-hydroxybenzoic acid), named GE/poly(3-HBA), and graphite electrode modified with electrochemically reduced graphene oxide and poly(3-hydroxybenzoic acid), named GE/ERGO/poly(3-HBA), were characterized electrochemically using anionic potassium ferrocyanide/ferricyanide probe ($K_4[Fe(CN)_6]/K_3[Fe(CN)_6].3H_2O$, 5 mmol L^{-1}, containing 0.1 mol L^{-1} of KCl). For this, cyclic voltammetry was performed from −0.3 V to +0.7 V, 50 mV s^{-1}. Atomic force microscopy and scanning electron microscopy were used to characterize the surface of the electrodes. The stability of the ERGO/poly(3-HBA) was also evaluated for 180 days, with the electrodes stored at −8 °C, aiming the evaluation of the charge involved in the oxidation process of the polymer film analysed by cyclic voltammetry every 15 days.

2.4. Cell lysate from A. acidoterrestris

Lyophilized *A. acidoterrestris* culture was solubilized in 100 mL of *Bacillus acidocaldarius* culture medium [46] and incubated at 40 °C for 48 h. After bacterial growth, the medium was centrifuged at 5000 rpm for 10 min. The supernatant was discarded and the precipitate was washed with 1 mL of Tris-EDTA buffer solution, centrifuged again at 5000 rpm for 10 min, and the pellet was resuspended in 100 mL of Tris-EDTA buffer solution. In sequence, 50 μL of sodium dodecyl sulfate solution (SDS, 10%) was added, followed by incubation for 30 min at 65 °C for the breaking of the bacterial membrane and genomic DNA exposure. The lysate was centrifuged (11,000 rpm, 15 min) and the supernatant was discarded. The precipitate was solubilized in 100 μL of Tris-EDTA buffer solution and stored at −8 °C until the moment of use. This solution was called positive control (PC), and the genomic DNA was quantified using a BioDrop spectrophotometer. A solution of *Escherichia coli* genomic DNA, purified in ABBOTT m2000sp extractor, was used as negative control (NC). Both positive and negative solutions were diluted to 120 μg mL^{-1} in saline-sodium citrate buffer solution (0.03 mol L^{-1} sodium citrate, 0.3 mol L^{-1} NaCl, adjusted to pH 7.0 with citric acid).

2.5. Orange juice samples

A sample of concentrated orange juice (65° Brix) was obtained from the Empresa Brasileira de Bebidas e Alimentos (Araguari, MG, Brazil). It was diluted in 5% (v/v) sodium phosphate buffer solution and autoclaved to ensure sterility. After this, the *A. acidoterrestris* cell lysate solution (PC) and the *E. coli* genomic DNA (NC) were diluted in the juice in the proportion of 1:1,000 and submitted to thermal denaturation at 98 °C for 5 min immediately before use for separation of the DNA strands.

2.6. Genosensor construction

Scheme 1 shows the steps of the electrode modification and biomolecules addition.

Specific oligonucleotides for *A. acidoterrestris,* ALIC1 (probe) and ALIC2 (target), were diluted in saline sodium citrate buffer (0.03 mol L^{-1}, NaCl 0.3 mol L^{-1}, pH 7.0) in the concentration of 100 μmol L^{-1} for both. Bovine serum albumin (BSA) blocking solution (0.5%, w/v) was prepared using sodium phosphate buffer solution. Initially, 15 μL of the ALIC1 solution were dripped onto the working electrodes and kept at 37 °C for 20 min to promote the adsorption of the oligonucleotide on the modified surface. Adsorption was used as it is fast and inexpensive, and previous works showed that small DNA molecules can be sucefully incorpored in electropolymerized polymers by this technique [34,43,47]. After this step, the electrode was washed by immersion in sodium phosphate buffer solution under agitation for 6 s, to remove probes that were not completely adsorbed. This washing process was the same for the subsequent steps. Then, 30 μL of BSA solution were dripped onto the electrodes and incubated at 37 °C for 60 min. Bovine serum albumin acts as surface blocker, preventing the target to be added from being adsorbed on the free surface of the electrode. After blocking, the electrode was washed again to remove excess BSA and dried with ultrapure nitrogen. Immediately before its use, the genosensor was kept at 70 °C for 3 min, to avoid a sudden decrease in temperature of the previously heated target solutions. The construction steps of the genosensor were monitored by electrochemical impedance spectroscopy (EIS; frequency range from 10000 Hz to 0.1 Hz, open circuit potential, amplitude 10 mV, quiet time 10 s) in an Autolab PGSTAT302N potentiostat (Netherlands) with a FRA2 module, using the anionic pair $K_4[Fe(CN)_6]/K_3[Fe(CN)_6]$ (5 mmol L^{-1}) in KCl solution (0.1 mol L^{-1}). The resistance to charge transfer (R_{ct}) values were calculated by the Nova 2.1.3 software, fitting the experimental data of the Nyquist plots in the equivalent circuit, with a $\chi^2 < 10^{-2}$.

2.7. Electrochemical detections

First, 15 μL of the target solution (ALIC2 solution, cell lisate or contaminated orange juice) were dripped onto the electrode surface, kept at 70 °C for 15 min for hybridization of the complementary DNA strands. This temperature was chosen because it is the annealing temperature of the used sequence. To construct a calibration curve, the *A. acidoterrestris* cell lysate was diluted in the following dilutions: 1:10, 1:100, 1:1,000 and 1:10,000. An undiluted sample was also used. For the direct electrochemical detection, the oxidation peak of the guanine base residue [48] was monitored by differential pulse voltammetry (+0.8 V at +1.2 V, 20 mV s^{-1}, amplitude 50 mV) in sodium phosphate buffer solution. For the indirect detection, after the drying of the genosensor incorporated with the target, 15 μL of a solution of Hoechst 33258 (20 μmol L^{-1}) were dripped on the elctrode and it was incubated at room temperature (25 °C) for 15 min, followed by washing. The oxidation peak of Hoechst 33258 was monitored [29] using differential pulse voltammetry (+0.35 V to +0.65 V, 20 mV s^{-1}, amplitude 50 mV) in sodium phosphate buffer solution. The shelf life of the genosensor was evaluated, in which the electrodes modified with DNA probe and blocked with BSA were stored at 4 °C for 70 days and analysed by differential pulse voltammetry every week, with an *A. acidoterrestris* lysate solution.

2.8. Data treatment

All electrochemical experiments were conducted in triplicate and the numerical results were presented in the arithmetic mean ± standard deviation format. Only standard deviations below 10% of the mean were considered acceptable. The final differential pulse voltammograms were subtracted from their respective baselines (voltammograms obtained under the same conditions, only in supporting electrolyte and without biomolecules) and the peaks were corrected by subtraction of a straight-line tangent to the base. The electrical charge envolved in the system were obtained by integrating the oxidation peaks of the voltammograms in function of time.

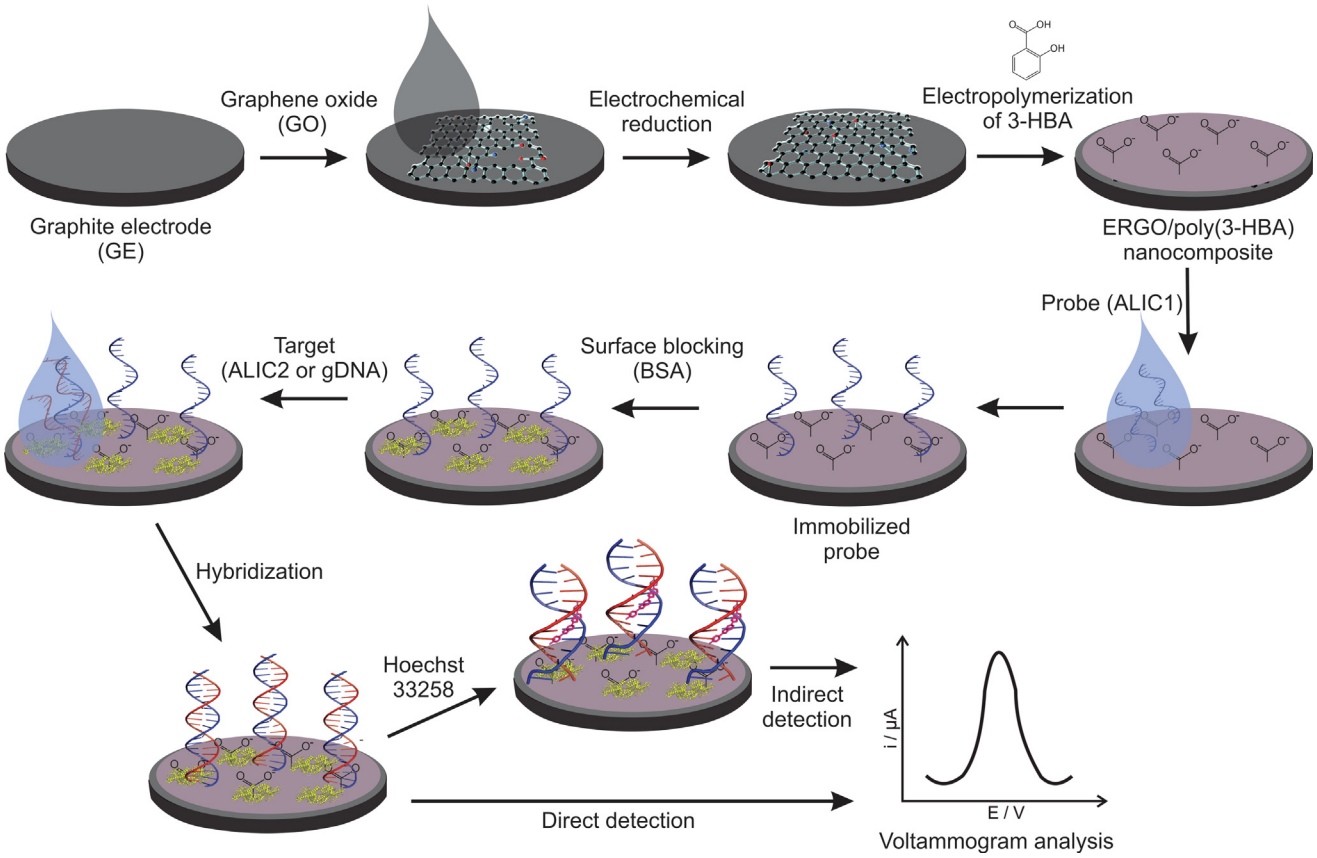

Scheme 1. Illustration of the construction steps of the genosensor. The orientation of the DNA molecule is mere illustrative.

3. Results and discussion

3.1. Graphite electrode modification with ERGO

Fig. 1A shows the cyclic voltammogram of the electrochemical reduction of graphene oxide on the surface of the graphite electrode in sodium phosphate buffer solution. The inset shows the comparison of the first reduction potential cycle for the electrode with and without modification.

It can be observed that the voltammogram for the bare GE does not show any reduction or oxidation peak, but the GE/GO shows a reduction peak at −1.3 V, due to the reduction of functional groups present in graphene oxide [49]. The second potential scan shows no noticeable peak, indicating that there was an irreversible reduction and a decrease in the amount of reducible functional groups of graphene oxide functional groups during the first potential scan. Fig. 1B shows the infrared spectra of the GE, GE/GO and GE/ERGO. The graphite electrode showed bands of low intensity in the region of aromatic rings (1640 cm^{-1}), characteristic of this material. The electrode modified with GO presented a wide and intense band in the region from 3700 cm^{-1} to 2750 cm^{-1}, atributted to hydroxyl groups. Other functional groups were also observed, displaying stretching peaks at 1720 cm^{-1} and 1210 cm^{-1}, relative to carbonyl and epoxides groups, respectively [50]. After the electrochemical reduction, differences in the spectra were observed, since there was a decrease in the absorption peaks in the previously mentioned regions, indicating that part of the oxygenated groups were removed from the material. Fig. 1C shows the cyclic voltammograms of the GE, GE/GO and GE/ERGO in aqueous solution of anionic probe. It can be observed that the GE has well-defined redox peaks for the pair $[Fe(CN)_6]^{3-/4-}$. For the GE/GO, a decrease of about five times in peak currents was observed, in relation to the profile of the bare graphite electrode. This decrease is due that the graphene oxide structure has insulating properties and oxygen functional groups that promotes the electronic repulsion of the $[Fe(CN)_6]^{3-/4-}$ redox pair [51]. After the reduction of the graphene oxide, the current values increased significantly, indicating an increase in the conductivity of the material, evidencing that the ERGO presents better electron transfer properties than the GO.

3.2. Electropolimerization of 3-hydroxybenzoic acid

Fig. 2A and 2B show the cyclic voltammograms of GE and GE/ERGO, respectively, for electropolymerization of 3-hydroxybenzoic acid.

In the cyclic voltammograms showed in Fig. 2A and 2B, the oxidation and reduction peaks of the polymer (indicated by the smaller arrows on the left) are increasing with successive potential scans, indicating the coverage of the surface by an electroactive material. On the other hand, the oxidation potential of the monomer (indicated by the large arrow on the right) shows lower values of electrical current, indicating its consumption. The addition of the ERGO promoted a monomer oxidation current peak of 1.8 mA, approximately 2.2 times higher than the unmodified electrode (0.8 mA). In addition, the oxidation potential of the monomer in the bare GE occurs in +1.12 V, and in the electrode modified with ERGO occurs in +1.03 V. This difference of 90 mV indicates that the nanomaterial facilitates the electron transfer in the oxidation process of the monomer, favoring the electropolymerization.

Fig. 2C shows the final electrochemical profile of the cyclic voltammograms of the GE/poly(3-HBA) and the GE/ERGO/poly(3-HBA) in support electrolyte solution. In presence of electrochemically reduced graphene oxide, the formation of the poly(3-hydroxybenzoic acid) promotes an increase in current when com-

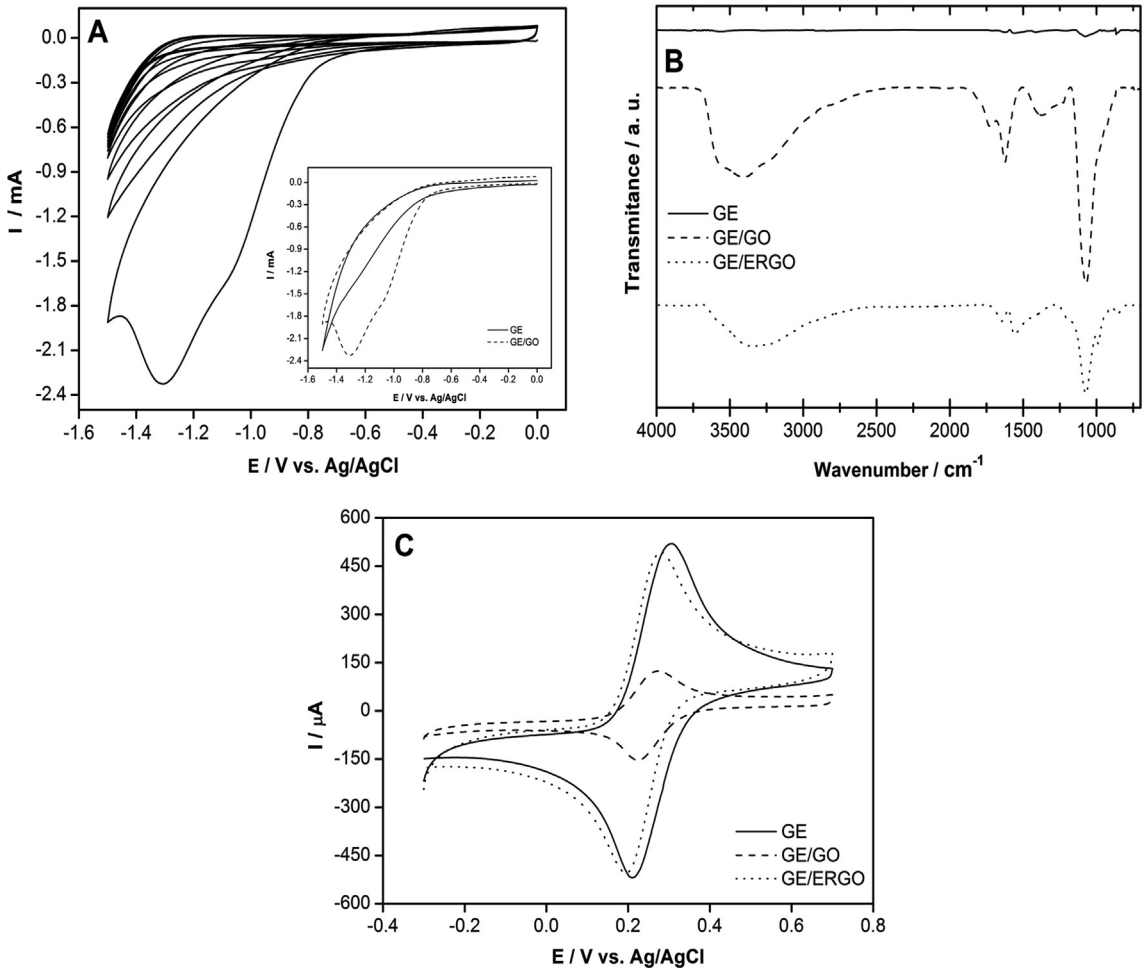

Fig. 1. Graphene reduction: (**A**) cyclic voltammogram of the electrochemical reduction of graphene oxide on the surface of the graphite electrode in sodium phosphate buffer solution (10 potential cycles, 50 mV s^{-1}). The inset shows the comparison of the first reduction potential cycle for the electrode with graphene oxide (GE/GO) and without modification (GE); (**B**) infrared spectra of the graphite electrode (GE), graphene electrode modified with graphene oxide (GE/GO) and graphene electrode modified with electrochemically reduced graphene oxide (GE/ERGO); (**C**) cyclic voltammograms of the graphite electrode (GE), graphene electrode modified with graphene oxide (GE/GO) and graphite electrode modified with electrochemically reduced graphene oxide (GE/ERGO) in aqueous solution of anionic probe ($K_4[Fe(CN)_6]/K_3[Fe(CN)_6].3H_2O$] (5 mmol L^{-1}) and KCl (0.1 mol L^{-1}), 50 mV s^{-1}).

pared to the electrode without the ERGO. This increase occurs mainly in the oxi-reduction electric potentials of the polymer material (between +0.3 V and +0.9 V), with a pronounced oxidation peak in +0.55 V and a reduction peak in +0.45 V. These results indicate that the nanomaterial ERGO contributes to the formation of more electroactive material derived from the 3-hydroxybenzoic acid. There is also an increase in the capacitive current, possibly due to the polymer's oxygenated groups, which facilitate the generation of the double electrical layer on the electrode surface in the aqueous solution. Fig. 2D shows a bar chart of the electrical charge, where a great difference is observed between the electrodes, since the amount of charge of the material formed using GE/ERGO as electrode is 5 times greater, thus reiterating the advantage of using ERGO as a base for the polymerization of the monomer.

Fig. 2E shows cyclic voltammograms for GE, GE/poly(3-HBA) and GE/ERGO/poly(3-HBA) in solution containing the anionic probes $[Fe(CN)_6]^{3-}/^{4-}$. In presence of the poly(3-hydroxybenzoic acid) there is a decrease in current values in relation to the profile of the redox probes on the graphite electrode, due to the structure of poly(3-hydroxybenzoic acid), presenting free carboxylate groups in this pH, promoting repulsion of the anionic probes. As previously shown, electrochemically reduced graphene oxide promotes an increase in the amount of poly(3-hydroxybenzoic acid), also resulting in an increase in the number of functional groups. Thus, the repulsion of the anionic probe is more pronounced, promoting the reduction of the current values.

Stability study of the modified electrode GE/ERGO/poly(3-HBA) is demonstrated in Fig. 2F, indicating the electric charge of the stored electrodes. After 180 days, the electrode maintened 78% of its electroactivity, thus is attractive for the construction of devices that demand storage time.

3.3. Morphological charactherization of the electrodes

Graphite electrode showed a typical rough surface (Fig. 3A) in SEM and AFM images (Rq = 84.7 ± 5.4 nm), while the GE/poly(3-HBA), Fig. 3B, showed large clusters on the surface and increase in roughness (Rq = 280.1 ± 17.2 nm), corresponding to the electropolymerized material. However, the GE/ERGO/poly(3-HBA) showed a smoother surface (Fig. 3C, Rq = 77.3 ± 6.7 nm), indicating that the reduced graphene oxide creates a more homogeneous substract for the electropolymerization of the 3-hydroxybenzoic acid, without the presence of large clusters of polymers.

3.4. Platform characterization by EIS

Electrochemical impedance spectroscopy is a valuable technique for electrochemical characterization of surfaces and can be

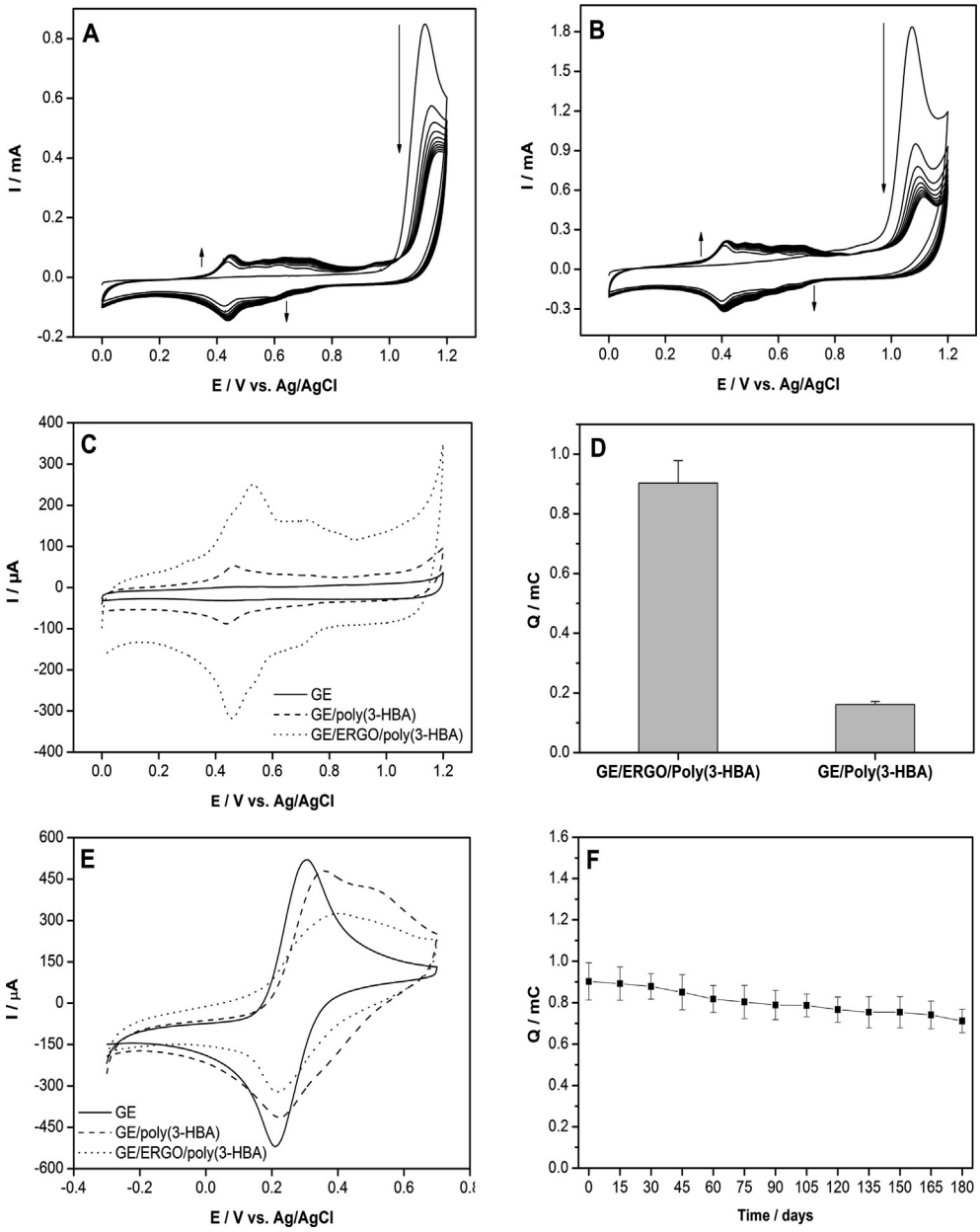

Fig. 2. Synthesis and characterization of GE/ERGO/poly(3-HBA): (**A**) cyclic voltammogram of the electropolymerization of 3-hydroxybenzoic acid (2.5 mmol L^{-1}) in $HClO_4$ solution (0.5 M), in the graphite electrode, 10 potential cycles, 50 mV s^{-1}; (**B**) cyclic voltammogram of the electropolymerization of 3-hydroxybenzoic acid (2.5 mmol L^{-1}) in $HClO_4$ solution (0.5 mol L^{-1}), in the graphite electrode modified with electrochemically reduced graphene oxide, 10 potential cycles, 50 mV s^{-1}; (**C**) cyclic voltammograms of the graphite electrode (GE), graphite electrode modified with poly(3-hydroxybenzoic acid) [GE/poly(3-HBA)] and graphite electrode modified with the electrochemically reduced graphene oxide and poly(3-hydroxybenzoic acid) [GE/ERGO/poly(3-HBA)] in $HClO_4$solution (0.5 mol L^{-1}), 50 mV s^{-1}; (**D**) bar chart showing the electric charge involved in the oxidation peaks of the poly(3-HBA) in the graphite electrode (GE) and the graphite electrode modified with electrochemically reduced graphene oxide (GE/ERGO); (**E**) cyclic voltammograms for GE, GE/poly(3-HBA) and GE/ERGO/poly(3-HBA) in aqueous solution of anionic probe ($K_4[Fe(CN)_6]/K_3[Fe(CN)_6].3H_2O$] (5 mmol L^{-1}) and KCl (0.1 mol L^{-1}), 1 potential cycle, 50 mV s^{-1}. (**F**) Graph showing the stability over time of GE/ERGO/poly(3-HBA).

used to monitor changes in the resistance to charge transfer in electrodes surface. Fig. 4A shows the Nyquist plots of the EIS analysis at each stage of the electrode modification, while Fig. 4B shows a bar chart with the calculated values of resistance to charge transfer (R_{ct}). The bare graphite electrode presented an average R_{ct} of 882 Ω. After the electrochemical reduction of graphene oxide on its surface, the R_{ct} increased to 1078 Ω, and the electropolymerization of 3-hydroxybenzoic acid improved this value to 1169 Ω. These resistance increases can be explained by the presence of unreduced oxygenated groups in the RGO and also by the existence of deprotonated carboxylic acid groups in the polymer structure, which repels $[Fe(CN)_6]^{3-}/^{4-}$ ions, due to the presence of the negative charges. The incorporation of the DNA probe increased the R_{ct} value to 1520 Ω, indicating that the attachment of the DNA probe by adsorption onto the electrode was successive, and it remains after the washing steps. The increase in the charge transfer resistance in this case can be explained by two factors: the presence of the DNA phosphate groups, which have a negative charge, thus repelling the ferrocyanide ions; and the inherent steric impediment of the presence of the biomolecule on the electrode surface [52]. Similarly, blocking the electrode surface with BSA also increases the resistence (R_{ct} = 2043 Ω), which is expected because the protein occupies the empty spaces on the electrode surface, in order to avoid unspecified interactions. Finally, after interacting

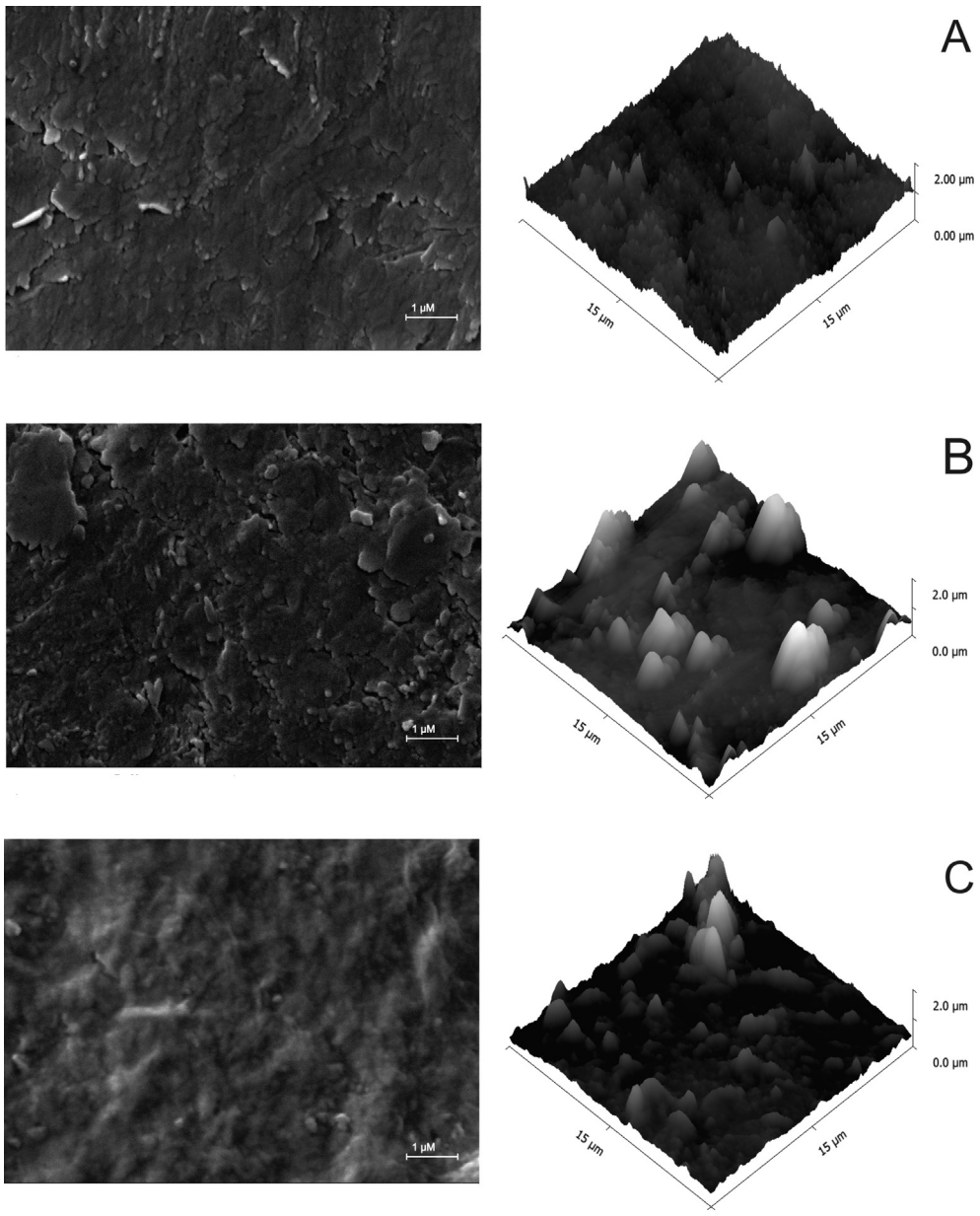

Fig. 3. Morphological characterization: (**A**) scanning electron microscopy (SEM) and atomic force microscopy (AFM) images of the graphite electrode; (**B**) SEM and AFM images of the graphite electrode modified with poly(3-hydroxybenzoic acid); (**C**) SEM and AFM images of the graphite electrode modified with the electrochemically reduced graphene oxide and poly(3-hydroxybenzoic acid).

the DNA probe (ALIC 1) with the complementary DNA target (ALIC 2), a new increase in resistance was observed (R_{ct} = 2254 Ω), indicating that the hybridization of the complementary DNA strands was successive, due to the increase in the quantity of biomolecules on the electrode surface that makes the electronic transfer even more difficult [53].

3.5. Direct and indirect detection of the target ALIC2

The oxidation peak of the ALIC DNA probe in Fig. 4C around +1.0 V, corresponding the region of the oxidation of the guanine nitrogenous base, indicates that the incorporation of the DNA probe was effective. Previous works with negative net charge polymers have demonstrated that a greater amount of DNA probe is adsorbed on the surface of the modified electrode in comparison with the bare electrode [42,54], despite the DNA phosphate group negative charges as well the polymer carboxylic acid group negative charge in pH 7. In the case of this work, as the DNA attachment is not oriented, its free coil-like structure allows any atoms of the molecule to interact with the nanomaterial, which also includes the atoms of the nitrogenous bases, that can interact with the polymer by hydrogen bonds, dipole–dipole and Van der Waals forces. After incubation with the target, it was observed a 2-fold decrease in the guanine oxidation peak current values. This reduction characterizes the hybridization process of the complementary oligonucleotides, as the formation of the hydrogen bonds of the double helix makes difficult to oxidize the residues of the nitrogenous bases present in the oligonucleotides, promoting a decrease in current values [16,55]. Fig. 4D shows the differential pulse voltamograms of the GE/ERGO/poly(3-HBA) in phosphate buffer solution, in the indirect detection of the ALIC2 oligonucleotide, by the presence of the Hoechst 33258 molecule. An increase of 3.6 times was observed in the current values in the region corresponding to the oxidation of the Hoechst 33258 indicator (+0.5 V), after incubation

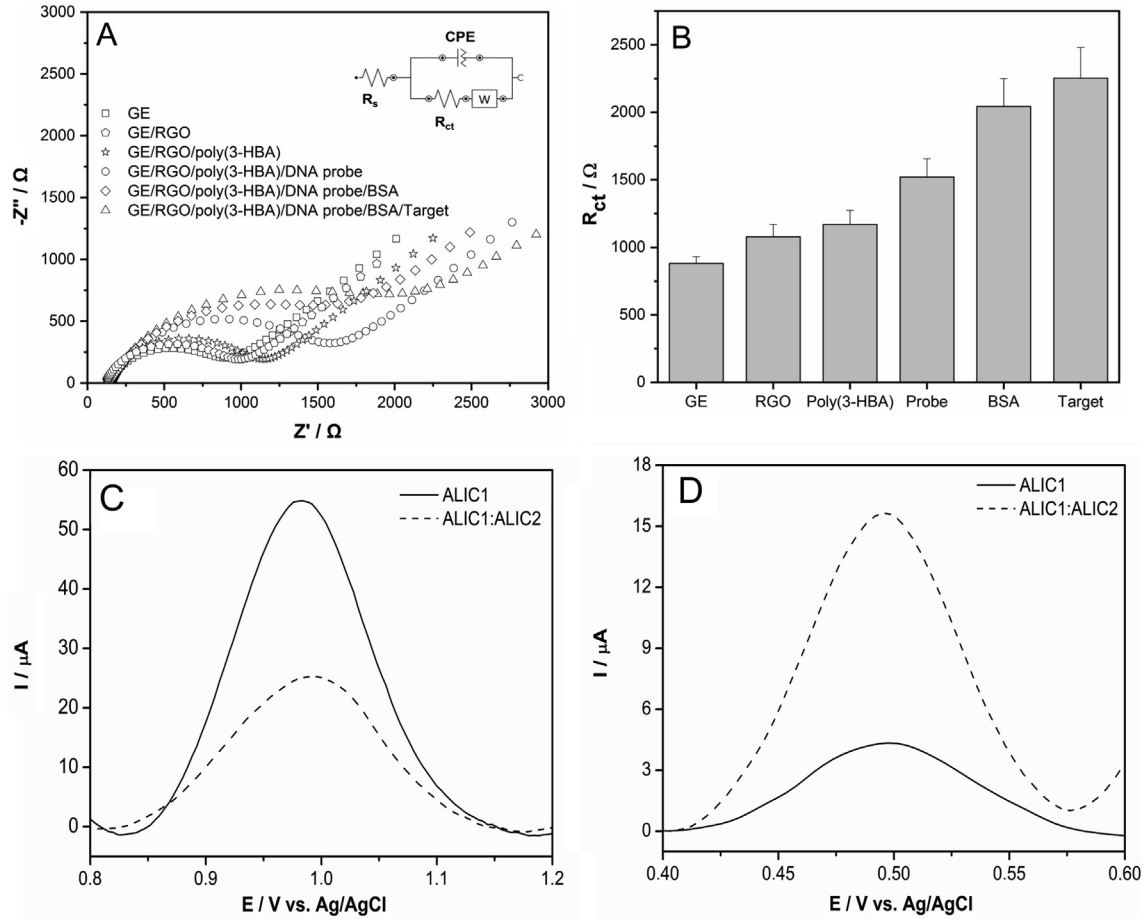

Fig. 4. EIS characterization and detection of complementary target: (**A**) nyquist plots obtained by EIS analisys in each genosensor construction step; inset: equivalent circuit, where R_s, R_{ct}, W, and CPE represent the solution resistance, the charge-transfer resistance, the Warburg diffusion resistance, and the constant phase element, respectively; (**B**) bar chart of the calculated R_{ct} values (n = 3) in the genosensor construction steps; electrolyte: KCl solution (0.1 mol L^{-1}), containing $K_4[Fe(CN)_6]$ and $K_3[Fe(CN)_6]$ (5 mmol L^{-1}), frequency range from 10000 Hz to 0.1 Hz, open circuit potential, amplitude 10 mV, quiet time 10 s; (**C**) differential pulse voltamograms (baseline subtracted) of the GE/ERGO/poly(3-HBA) incorporated with the probe (ALIC1) in sodium phosphate buffer solution (+0.8 V to + 1.2 V, 20 mV s^{-1}, amplitude 50 mV) relative to the direct detection of *A. acidoterrestris* target oligonucleotide (ALIC2); (**D**) differential pulse voltamograms (baseline subtracted) of the GE/ERGO/poly(3-HBA) incorporated with the probe (ALIC1) in phosphate buffer solution (0.1 mol L^{-1}), pH 7.4, relative to the indirect detection of *A. acidoterrestris* target oligonucleotide (ALIC2), 20 mV s^{-1}, amplitude 50 mV. ALIC1 and ALIC2 concentration: 100 μmol L^{-1}.

with the target. Hoechst 33258 is a DNA minor groove binding, with high affinity for the double helix [56], thus it remains retained on the electrode after washing, monitoring the hybridization process by detecting the complementary strand. The advantage of this methodology in relation to direct detection is the possibility of detecting the complementary target in more cathodic potentials, preventing oxidation of possible interfering substances. We can also report a higher sensitivity in indirect detection since the current difference between probe and target was higher than the direct detection.

3.6. Detection of the genomic DNA of A. acidoterrestris and calibration curve

After incubation of the genosensor with the *A. acidoterrestris* cell lysate, it was observed an increase in the current peak of 5.5 times in the region corresponding to the oxidation of the Hoechst 33258 indicator (Fig. 5A), compared to the probe. As the indicator has affinity for the double-stranded DNA, it remains on the surface of the electrode after washing, monitoring the hybridization process by detecting the complementary strand. The genosensor was also able to discern different species, since the oxidation peak current value of the minor-groove binder in the presence of the negative control (*E. coli* genomic DNA) is 2.5 times less than the current value obtained with the positive control. The small retention of Hoechst 33258 in the absence of complementary DNA on the electrode surface can be explained by the planar structure of the bisbenzimide molecule, which can interact by Van der Waals forces with with the aromatic rings presented in the nanocomposite structure.

Indirect detection of the genomic DNA present in *A. acidoterrestris* cell lysate at different dilutions is showed in Fig. 5B. The concentration of genomic DNA in each diluition were as follows: 120 μg mL^{-1} (no diluition), 12 μg mL^{-1} (1:10), 1.2 μg mL^{-1} (1:100), 120 ng mL^{-1} (1:1,000) and 12 ng mL^{-1} (1:10,000). The calibration curve of the genosensor was constructed (Fig. 5C), as the oxidation peak current of the Hoechst 33258 indicator correlates with the logarithm of the concentration of genomic DNA of *A. acidoterrestris*. A decrease in the oxidation peak current was observed after subsequent dilutions of the sample of *A. acidoterrestris*. The experimental calibration curve can be fitted by a linear straight line of equation: ip (μA) = 4.551 (μA $μg^{-1}$ mL^{-2}) . log[gDNA] (μg mL^{-1}) + 13.841 (μA), r = 0.993, RSD = 1.9% (n = 3). The assumed limit of detection was the lowest DNA concentration that had a significantly higher response than the blank, which was 12 ng mL^{-1} (1:10,000 diluition).

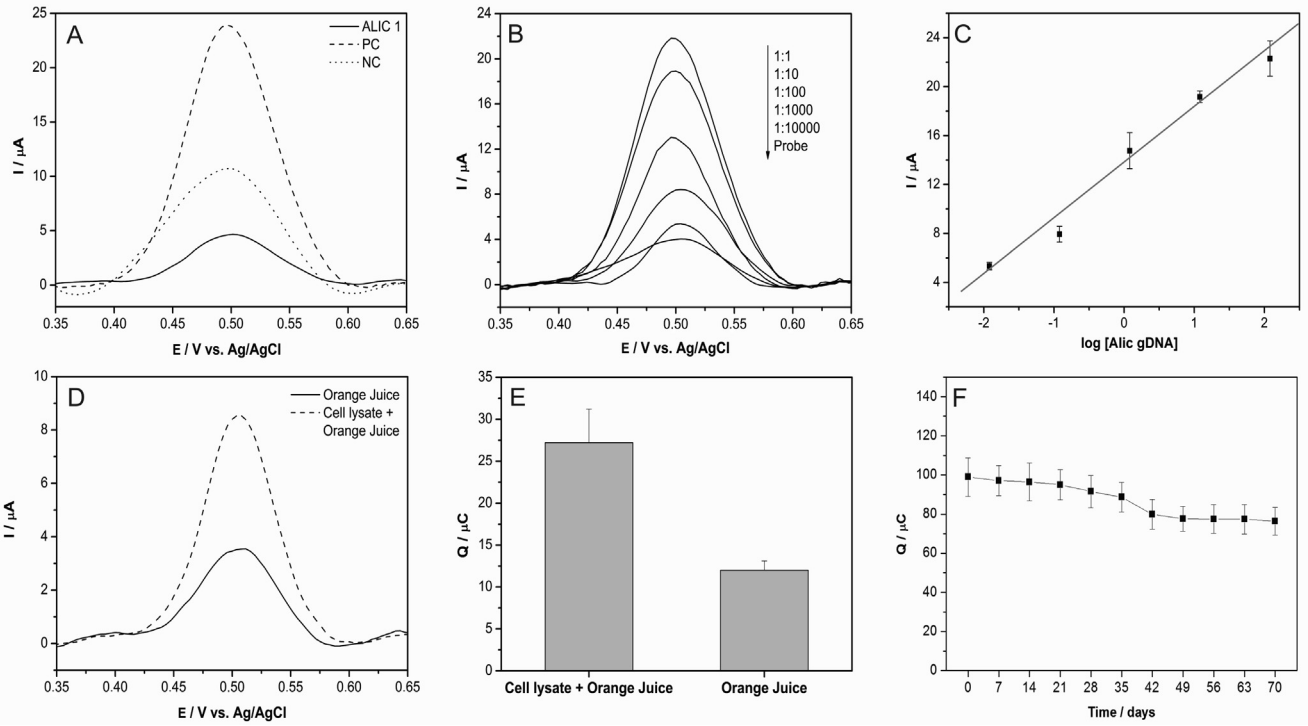

Fig. 5. Detection of genomic DNA: (**A**) differential pulse voltamograms (baseline subtracted) of the GE/ERGO/poly(3-HBA) with the probe (ALIC1), indirect detection of the *A. acidoterrestris* genomic DNA in the cell lysate (120 μg mL^{-1}, positive control - PC) and *E. coli* genomic DNA (120 μg mL^{-1}, negative control - NC), 20 mV s^{-1}, amplitude 50 mV; (**B**) differential pulse voltamograms (baseline subtracted) of the GE/ERGO/poly(3-HBA) incorporated with the probe (ALIC1) of the indirect detection of genomic DNA present in *A. acidoterrestris* cell lysate at different dilutions, 20 mV s^{-1}, amplitude 50 mV; (**C**) calibration curve of the genosensor, where the oxidation peak current of the Hoechst 33258 indicator is correlated with the logarithm of the concentration of the genomic DNA present in the *A. acidoterrestris* cell lysate; (**D**) differential pulse voltamograms (baseline subtracted) of GE/ERGO/poly(3-HBA) incorporated with the probe (ALIC1) in sodium phosphate buffer solution, relative to the indirect detection of the *A. acidoterrestris* genomic DNA in orange juice contaminated with cell lysate, 20 mV s^{-1}, amplitude 50 mV; (**E**) bar chart showing the electric charge involved in the oxidation peak of the Hoechst 33258 intercalant in the indirect detection of the *A. acidoterrestris* genomic DNA in the orange juice contaminated with the cell lysate and in the sterile orange juice; (**F**) graph relating the charge of the Hoechst 33258 oxidation process with the storage days of the genosensor in the detection of *A. acidoterrestris* genomic DNA in cell lysate.

Previous studies have also demonstrated the use of Hoechst 33,258 as an electrochemical indicator of DNA hybridization, but employing small DNA sequences as targets [27,30]. In this study the whole bacterial DNA was used, which gives the biosensor greater practicality, requiring no additional sample treatment steps such as DNA fragmentation by restriction enzymes or polymerase chain reaction amplification.

Ensuring that the components of the orange juice does not affect the hybridization process neither the oxidation of the electroactive indicator, in the orange juice artificially contaminated with the cellular lysate of *A. acidoterrestris* a higher oxidation peak and resultant charge of Hoechst 33258 is noted in the presence of the *A. acidoterrestris* bacterial cell lysate (Fig. 5D and 5E), a 2.5-fold difference than the sterile orange juice. As the orange juice is a complex sample and has electroactive components that can interfere with electrochemical detection (such as ascorbic acid and citric acid), the proposed detection method was effective.

The stability of a biosensor is an important factor in determining its future commercialization, and this parameter is often overlooked in studies. Fig. 5F shows the study of the shelf life of the genosensor, indicating that the genosensor maintained 77% of its activity after 70 days, and in the first 35 days the charge of the Hoechst 33258 oxidation peak remained practically constant, decreasing in the subsequent days. Considering the total assay time (70 days) and the storage conditions (4 °C, dry chamber, atmospheric air), as well as the use of biomolecules such as DNA and BSA, the genosensor presented good response. The electropolymerized nanomaterial creates a porous matrix with a large surface area, capable of retaining water even in dry conditions [44]. The presence of water is essential in maintaining the native and functional conformation of biomolecules, including DNA, thus creating a more stable environment for the biomolecule. At the end of the seventieth day, the genosensor was still able to recognize the target in samples of cell lysate, indicating its suitability for use after a long period of storage. Nanocomposites assembled by reduced graphene oxide in combination with other nanomaterials for electrochemical DNA detection are present in the literature [57–59]. The added value of the strategy showed in this work is that it allows both RGO and polymer to be obtained by electrochemical techniques and directly on the electrode surface, without the need of material purification, post-deposition or the use of expensive and harmful reagents, in a short time and with an inexpensive method.

There is a lack of studies in the literature reporting biosensors for the detection of *A. acidoterrestris*. Eguiluz and coworkers [60] developed an electrode for detection of an RT-PCR product of *A. acidoterrestris*, but the RNA extraction process is laborious and expensive. In view of deficiency of description of other biosensors for detection of *A. acidoterrestris* genomic DNA, as well as the reported biosensor ease of use, requiring less sample treatment, restricted to obtaining the cell lysate, low detection limit and good stability, this genosensor is presented as a suitable platform for detection of *A. acidoterrestris*.

4. Conclusions

The results indicate that the genosensor developed with electrochemically reduced graphene oxide, poly(3-hydroxybenzoic

acid), a specific single-stranded DNA probe and employing Hoechst 33258 as indicator is a suitable device capable of detecting genomic DNA. In this work it was applied for the detection of *A. acidoterrestris*, however, by varying the sequence of the immobilized probe, the platform can be used to detect other microorganisms. Morphological and electrochemical characterizations demonstrated that the combined use of electrochemically reduced graphene oxide and the polymer derived from the 3-hydroxybenzoic acid resulted in an excellent platform for the construction of the bioelectrode. The calibration curve indicated that the genosensor has a response proportional to the logarithm of the analyte concentration, with detection limit of 12 ng mL^{-1}, and the use of Hoechst 33258 proved to be effective in the electrochemical detection of the hybridization event. The device also demonstrated a stability of 77% in 70 days of storage. The doping of orange juice with DNA lysate also demonstrated that the components of the juice matrix do not interfere with the oxidation of the electroactive indicator. These results show that this genosensor is a suitable platform for detection of *A. acidoterrestris*, aiming the certification of the quality of orange juice and its applicability in the juice production chain. This is also the first reported genosensor for detection of *A. acidoterrestris* total genomic DNA in the literature.

Declaration of Competing Interest

The authors declared that there is no conflict of interest.

Acknowledgements

The authors are grateful for the financial support from Conselho Nacional de Desenvolvimento Científico e Tecnológico (CNPq), Fundação de Amparo à Pesquisa do Estado de Minas Gerais (FAPEMIG) and Coordenação de Aperfeiçoamento de Pessoal de Nível Superior (CAPES).

References

[1] L. Helm, I.A. Macdonald, Impact of beverage intake on metabolic and cardiovascular health, Nutr. Rev. 73 (suppl 2) (2015) 120–129, https://doi.org/10.1093/nutrit/nuv049.
[2] D.F. Jesus, M.F. Leite, L.F.M. Silva, R.D. Modesta, V.M. Matta, L.M.C. Cabral, Orange (Citrus sinensis) juice concentration by reverse osmosis, J. Food Eng. 81 (2) (2007) 287–291, https://doi.org/10.1016/j.jfoodeng.2006.06.014.
[3] B.A. Osopale, G.A. Adewumi, R.C. Witthuhn, O.O. Kuloyo, F.A. Oguntoyinbo, A review of innovative techniques for rapid detection and enrichment of Alicyclobacillus during industrial processing of fruit juices and concentrates, Food Control 99 (2019) 146–157, https://doi.org/10.1016/j.foodcont.2018.12.032.
[4] U. Bagci, A. Temiz, Microbiological quality of fresh-squeezed orange juice and efficacy of fruit surface decontamination methods in microbiological quality, J. Food Prot. 74 (2011) 1238–1244, https://doi.org/10.4315/0362-028X.JFP-11-021.
[5] J.V. Alberice, M.E. Funes-Huacca, S.B. Guterres, E. Carrilho, Inactivation of Alicyclobacillus acidoterrestris in orange juice by saponin extracts combined with heat-treatment, Int. J. Food Microbiol. 159 (2) (2012) 130–135, https://doi.org/10.1016/j.ijfoodmicro.2012.08.004.
[6] R. Cai, Y. Yuan, Z. Wang, C. Guo, B. Liu, C. Pan, L. Liu, T. Yue, Effects of preservatives on Alicyclobacillus acidoterrestris growth and guaiacol production, Int. J. Food Microbiol. 214 (2015) 145–150, https://doi.org/10.1016/j.ijfoodmicro.2015.08.013.
[7] B.A. Osopale, C.R. Witthuhn, J. Albertyn, F.A. Oguntoyinbo, Culture dependent and independent genomic identification of Alicyclobacillus species in contaminated commercial fruit juices, Food Microbiol. 56 (2016) 21–28, https://doi.org/10.1016/j.fm.2015.11.014.
[8] T. Hünniger, C. Fischer, H. Wessels, A. Hoffmann, A. Paschke-Kratzin, I. Haase, M. Fischer, Food sensing: Selection and characterization of DNA aptamers to alicyclobacillus spores for trapping and detection from orange juice, J. Agric. Food Chem. 63 (8) (2015) 2189–2197, https://doi.org/10.1021/jf505996m.
[9] L. Guadarrama-Fernández, M. Novell, P. Blondeau, F.J. Andrade, A disposable, simple, fast and low-cost paper-based biosensor and its application to the determination of glucose in commercial orange juices, Food Chem. 265 (2018) 64–69, https://doi.org/10.1016/j.foodchem.2018.05.082.
[10] X. Jiang, S. Liu, M. Yang, A. Rasooly, Amperometric genosensor for culture independent bacterial count, Sensors Actuators, B Chem. 299 (2019) 126944, https://doi.org/10.1016/j.snb.2019.126944.
[11] M. Ligaj, M. Tichoniuk, D. Gwiazdowska, M. Filipiak, Electrochemical DNA biosensor for the detection of pathogenic bacteria Aeromonas hydrophila, Electrochim. Acta 128 (2014) 67–74, https://doi.org/10.1016/j.electacta.2013.10.061.
[12] K. Kashish, S. Gupta, S.K. Dubey, R. Prakash, Prakash, Genosensor based on a nanostructured, platinum-modified glassy carbon electrode for Listeria detection, Anal. Methods 7 (6) (2015) 2616–2622, https://doi.org/10.1039/C5AY00167F.
[13] L.E. Ahangar, M.A. Mehrgardi, Amplified detection of hepatitis B virus using an electrochemical DNA biosensor on a nanoporous gold platform, Bioelectrochemistry 117 (2017) 83–88, https://doi.org/10.1016/j.bioelechem.2017.06.006.
[14] E. Torelli, M. Manzano, R.S. Marks, Chemiluminescent optical fibre genosensor for porcine meat detection, Sensors Actuators, B Chem. 247 (2017) 868–874, https://doi.org/10.1016/j.snb.2017.03.064.
[15] L.M. Alves, V.R. Rodovalho, A.C.H. Castro, M.A.R. Freitas, C.M. Mota, T.W.P. Mineo, J.R. Mineo, J.M. Madurro, A.G. Brito-Madurro, Development of direct assays for Toxoplasma gondii and its use in genomic DNA sample, J. Pharm. Biomed. Anal. 145 (2017) 838–844, https://doi.org/10.1016/j.jpba.2017.07.050.
[16] J.I.A. Rashid, N.A. Yusof, The strategies of DNA immobilization and hybridization detection mechanism in the construction of electrochemical DNA sensor: A review, Sens. Bio-Sensing Res. 16 (2017) 19–31, https://doi.org/10.1016/j.sbsr.2017.09.001.
[17] S.H. Minasyan, L.A. Tavadyan, A.P. Antonyan, H.G. Davtyan, M.A. Parsadanyan, P.O. Vardevanyan, Differential pulse voltammetric studies of ethidium bromide binding to DNA, Bioelectrochemistry 68 (1) (2006) 48–55, https://doi.org/10.1016/j.bioelechem.2005.03.006.
[18] A.C. Honorato Castro, E.G. França, L.F. De Paula, M.M.C.N. Soares, L.R. Goulart, J. M. Madurro, A.G. Brito-Madurro, Preparation of genosensor for detection of specific DNA sequence of the hepatitis B virus, Appl. Surf. Sci. 314 (2014) 273–279, https://doi.org/10.1016/j.apsusc.2014.06.084.
[19] Z. Zhang, X. Zhao, J. Liu, J. Yin, X. Cao, Highly sensitive sandwich electrochemical sensor based on DNA-scaffolded bivalent split aptamer signal probe, Sensors Actuators, B Chem. 311 (2020) 127920, https://doi.org/10.1016/j.snb.2020.127920.
[20] D.A. Oliveira, J.V. Silva, J.M.R. Flauzino, A.C.H. Castro, A.C.R. Moço, M.M.C.N. Soares, J.M. Madurro, A.G. Brito-Madurro, Application of nanomaterials for the electrical and optical detection of the hepatitis B virus, Anal. Biochem. 549 (2018) 157–163, https://doi.org/10.1016/j.ab.2018.03.023.
[21] Y. Jin, X. Yao, Q. Liu, J. Li, Hairpin DNA probe based electrochemical biosensor using methylene blue as hybridization indicator, Biosens. Bioelectron. 22 (6) (2007) 1126–1130, https://doi.org/10.1016/j.bios.2006.04.011.
[22] R.P. Alves-Balvedi, L.P. Caetano, J.M. Madurro, A.G. Brito-Madurro, Use of 3,3',5,5' tetramethylbenzidine as new electrochemical indicator of DNA hybridization and its application in genossensor, Biosens. Bioelectron. 85 (2016) 226–231, https://doi.org/10.1016/j.bios.2016.05.016.
[23] P. Kittimongkolsuk, T. Tencomnao, R. Santiyanont, Semi-quantitative detection of gene expression using bisbenzimide dye, Genet. Mol. Res. (2011), https://doi.org/10.4238/2011.November.22.8.
[24] Q.-X. Wang, F. Gao, F. Gao, S.-X. Li, W. Weng, F.-Q. Liu, K. Jiao, A novel hybridization indicator for the low-background detection of short DNA fragments based on an electrically neutral cobalt(II) complex, Biosens. Bioelectron. 32 (1) (2012) 50–55, https://doi.org/10.1016/j.bios.2011.11.020.
[25] T. Stokke, H.B. Steen, Binding of Hoechst 33258 to chromatin in situ, Cytometry 7 (3) (1986) 227–234, https://doi.org/10.1002/cyto.990070302.
[26] U. Issar, T. Kumari, R. Arora, R. Kakkar, Conformational properties of DNA minor groove binder Hoechst 33258 in gas phase and in aqueous solution, Comput. Theor. Chem. 1113 (2017) 32–41, https://doi.org/10.1016/j.comptc.2017.05.006.
[27] M. Kobayashi, T. Kusakawa, M. Saito, S. Kaji, M. Oomura, S. Iwabuchi, Y. Morita, Q. Hasan, E. Tamiya, Electrochemical DNA quantification based on aggregation induced by Hoechst 33258, Electrochem. Commun. 6 (4) (2004) 337–343, https://doi.org/10.1016/j.elecom.2004.01.012.
[28] L.R. Ferguson, W.A. Denny, Microbial mutagenic effects of the DNA minor groove binder pibenzimol (Hoechst 33258) and a series of mustard analogues, Mutat. Res. - Fundam. Mol. Mech. Mutagen. 329 (1995) 19–27, https://doi.org/10.1016/0027-5107(95)00013-9.
[29] H. Zhao, Z. Li, N.Y. Lee, J.S. Kim, E.-C.-C. Lee, S.Y. Breusegem, P. Regenfuss, Electrochemical DNA detection using Hoechst dyes in microfluidic chips, Curr. Appl Phys. 12 (2012) 1493–1496, https://doi.org/10.1016/j.cap.2012.04.023.
[30] Y.-S. Choi, K.-S. Lee, D.-H. Park, Gene detection using Hoechst 33258 on a biochip, Curr. Appl Phys. 6 (4) (2006) 777–780, https://doi.org/10.1016/j.cap.2005.04.038.
[31] D.A. Oliveira, J.V. Silva, J.M.R. Flauzino, H.S. Sousa, A.C.H. Castro, A.C.R. Moço, M.M.C.N. Soares, J.M. Madurro, A.G. Brito-Madurro, Carbon nanomaterial as platform for electrochemical genosensor: A system for the diagnosis of the hepatitis C in real sample, J. Electroanal. Chem. 844 (2019) 6–13, https://doi.org/10.1016/j.jelechem.2019.04.045.
[32] M.K.L. da Silva, H.C. Vanzela, L.M. Defavari, I. Cesarino, Determination of carbamate pesticide in food using a biosensor based on reduced graphene oxide and acetylcholinesterase enzyme, Sensors Actuators, B Chem. 277 (2018) 555–561, https://doi.org/10.1016/j.snb.2018.09.051.
[33] J. Fu, X. An, Y. Yao, Y. Guo, X. Sun, Electrochemical aptasensor based on one step co-electrodeposition of aptamer and GO-CuNPs nanocomposite for

organophosphorus pesticide detection, Sensors Actuators, B Chem. 287 (2019) 503–509, https://doi.org/10.1016/j.snb.2019.02.057.
[34] R.P.A.A. Balvedi, A.C.H.H. Castro, J.M. Madurro, A.G. Brito-Madurro, Detection of a specific biomarker for epstein-barr virus using a polymer-based genosensor, Int. J. Mol. Sci. 15 (2014) 9051–9066, https://doi.org/10.3390/ijms15059051.
[35] Y. Aceta, M. del Valle, Graphene electrode platform for impedimetric aptasensing, Electrochim. Acta 229 (2017) 458–466, https://doi.org/10.1016/j.electacta.2017.01.113.
[36] M.J. Dunlop, R. Bissessur, Nanocomposites based on graphene analogous materials and conducting polymers: a review, J. Mater. Sci. 55 (16) (2020) 6721–6753, https://doi.org/10.1007/s10853-020-04479-9.
[37] P. Sobolewski, M. Piwowarczyk, M.E. Fray, Polymer-Graphene Nanocomposite Materials for Electrochemical Biosensing, Macromol. Biosci. 16 (7) (2016) 944–957, https://doi.org/10.1002/mabi.201600081.
[38] A. Ehsani, H. Mohammad Shiri, E. Kowsari, R. Safari, J. Torabian, S. Kazemi, Nanocomposite of p-type conductive polymer/functionalized graphene oxide nanosheets as novel and hybrid electrodes for highly capacitive pseudocapacitors, J. Colloid Interface Sci. 478 (2016) 181–187, https://doi.org/10.1016/j.jcis.2016.06.013.
[39] S. Song, Y. Zhai, Y. Zhang, Bioinspired Graphene Oxide/Polymer Nanocomposite Paper with High Strength, Toughness, and Dielectric Constant, ACS Appl. Mater. Interfaces 8 (45) (2016) 31264–31272, https://doi.org/10.1021/acsami.6b08606.
[40] S. Mao, H. Pu, J. Chen, Graphene oxide and its reduction: Modeling and experimental progress, RSC Adv. 2 (2012) 2643–2662, https://doi.org/10.1039/c2ra00663d.
[41] Z. Zhang, J. Yan, H. Jin, J. Yin, Tuning the reduction extent of electrochemically reduced graphene oxide electrode film to enhance its detection limit for voltammetric analysis, Electrochim. Acta 139 (2014) 232–237, https://doi.org/10.1016/j.electacta.2014.06.159.
[42] J.V. da Silva, A.G.B. Madurro, J.M. Madurro, Modified electrode with reduced graphene oxide/poly(3-hydroxyphenylacetic acid): a new platform for oligonucleotide hybridization, J. Solid State Electrochem. 21 (7) (2017) 2129–2139, https://doi.org/10.1007/s10008-017-3601-8.
[43] D.C. Ferreira, L.P. Rodrigues, J.M. Madurro, A.G.B. Madurro, R.T.S. de Oliveira, O. Abraha&tild;o, Graphite Electrodes Modified With Poly(3-Hydroxybenzoic Acid) for Oligonucleotides Sensors, Int. J. Electrochem. Sci. 9 (2014) 6246–6257.
[44] Deusmaque Carneiro Ferreira, Antonio Eduardo da Hora Machado, Fernanda de Souza Tiago, João Marcos Madurro, Ana Graci Brito Madurro, Odonírio Abrahão, Molecular modeling study on the possible polymers formed during the electropolymerization of 3-hydroxyphenylacetic acid, J. Mol. Graph. Model. 34 (2012) 18–27, https://doi.org/10.1016/j.jmgm.2012.01.001.
[45] William S. Hummers, Richard E. Offeman, Preparation of Graphitic Oxide, J. Am. Chem. Soc. 80 (6) (1958), https://doi.org/10.1021/ja01539a017.
[46] V. Buonocore, C. Caporale, M. De Rosa, A. Gambacorta, Stable, inducible thermoacidophilic α amylase from Bacillus acidocaldarius, J. Bacteriol. 128 (1976) 515–521, https://doi.org/10.1128/jb.128.2.515-521.1976.
[47] Ana Cristina Honorato de Castro, Leandro Toshio Kochi, Anna Clara Rios Moço, Roney S. Coimbra, Guilherme C. Oliveira, Sara Cuadros-Orellana, João Marcos Madurro, Ana Graci Brito-Madurro, A new genosensor for meningococcal meningitis diagnosis using biological samples, J. Solid State Electrochem. 22 (8) (2018) 2339–2346, https://doi.org/10.1007/s10008-018-3940-0.
[48] A.M. Oliveira-Brett, J.A.P. Piedade, L.A. Silva, V.C. Diculescu, Voltammetric determination of all DNA nucleotides, Anal. Biochem. 332 (2) (2004) 321–329, https://doi.org/10.1016/j.ab.2004.06.021.
[49] Elaine Lay Khim Chng, Martin Pumera, Solid-state electrochemistry of graphene oxides: Absolute quantification of reducible groups using voltammetry, Chem. - An Asian J. 6 (11) (2011) 2899–2901, https://doi.org/10.1002/asia.201100464.
[50] Juan Yang, Yazhou Zhou, Lei Sun, Nan Zhao, Chuanliang Zang, Xiaonong Cheng, Synthesis, characterization and optical property of graphene oxide films, Appl. Surf. Sci. 258 (12) (2012) 5056–5060, https://doi.org/10.1016/j.apsusc.2012.01.105.
[51] A.L. Liu, G.X. Zhong, J.Y. Chen, S.H. Weng, H.N. Huang, W. Chen, L.Q. Lin, Y. Lei, F.H. Fu, Z.L. Sun, X.H. Lin, J.H. Lin, S.Y. Yang, A sandwich-type DNA biosensor based on electrochemical co-reduction synthesis of graphene-three dimensional nanostructure gold nanocomposite films, Anal. Chim. Acta 767 (2013) 50–58, https://doi.org/10.1016/j.aca.2012.12.049.
[52] J. Zhang, D. Han, R. Yang, Y. Ji, J. Liu, X. Yu, Electrochemical detection of DNA hybridization based on three-dimensional ZnO nanowires/graphite hybrid microfiber structure, Bioelectrochemistry 128 (2019) 126–132, https://doi.org/10.1016/j.bioelechem.2019.04.003.
[53] Marines Steinmetz, Dhésmon Lima, Adriano Gonçalves Viana, Sérgio Toshio Fujiwara, Christiana Andrade Pessôa, Rafael Mazer Etto, Karen Wohnrath, A sensitive label-free impedimetric DNA biosensor based on silsesquioxane-functionalized gold nanoparticles for Zika Virus detection, Biosens. Bioelectron. 141 (2019) 111351, https://doi.org/10.1016/j.bios.2019.111351.
[54] T. a. R. Silva, L.F. Ferreira, L.M. Souza, L.R. Goulart, J.M. Madurro, A.G. Brito-Madurro, New approach to immobilization and specific-sequence detection of nucleic acids based on poly(4-hydroxyphenylacetic acid), Mater. Sci. Eng. C. 29 (2009) 539–545. doi:10.1016/j.msec.2008.09.048.
[55] F.B. Silva, S.N. Vieira, L.R.G.G. Filho, J.F.C.C. Boodts, A.G. Brito-Madurro, J.M. Madurro, L.R. Goulart, J.F.C.C. Filho, A.G. Boodts, J.M. Brito-Madurro, L.R.G.G. Madurro, J.F.C.C. Filho, A.G. Boodts, J.M. Brito-Madurro, L.R. Goulart Madurro, J. F.C.C. Filho, A.G. Boodts, J.M. Brito-Madurro, L.R.G.G. Madurro, J.F.C.C. Filho, A. G. Boodts, J.M. Madurro Brito-Madurro, Electrochemical investigation of oligonucleotide-DNA hybridization on poly(4-methoxyphenethylamine), Int. J. Mol. Sci. 9 (2008) 1173–1187, https://doi.org/10.3390/ijms9071173.
[56] Philip E. Pjura, Kazimierz Grzeskowiak, Richard E. Dickerson, Binding of Hoechst 33258 to the minor groove of B-DNA, J. Mol. Biol. 197 (2) (1987) 257–271, https://doi.org/10.1016/0022-2836(87)90123-9.
[57] Y. Wang, H. Sauriat-Dorizon, H. Korri-Youssoufi, Direct electrochemical DNA biosensor based on reduced graphene oxide and metalloporphyrin nanocomposite, Sensors Actuators, B Chem. 251 (2017) 40–48, https://doi.org/10.1016/j.snb.2017.04.128.
[58] Siva Kumar Krishnan, Eric Singh, Pragya Singh, Meyya Meyyappan, Hari Singh Nalwa, A review on graphene-based nanocomposites for electrochemical and fluorescent biosensors, RSC Adv. 9 (16) (2019) 8778–8881, https://doi.org/10.1039/C8RA09577A.
[59] Zhihong Zhang, Xiaoming Fu, Kunzhen Li, Ruixue Liu, Donglai Peng, Linghao He, Minghua Wang, Hongzhong Zhang, Liming Zhou, One-step fabrication of electrochemical biosensor based on DNA-modified three-dimensional reduced graphene oxide and chitosan nanocomposite for highly sensitive detection of Hg(II), Sensors Actuators, B Chem. 225 (2016) 453–462, https://doi.org/10.1016/j.snb.2015.11.091.
[60] Katlin Ivon Barrios Eguiluz, Giancarlo Richard Salazar-Banda, Maribel Elizabeth Funes-Huacca, Juliana Vieira Alberice, Emanuel Carrilho, Sergio Antonio Spinola Machado, Luis Alberto Avaca, Sequence-specific electrochemical detection of Alicyclobacillus acidoterrestris DNA using electroconductive polymer-modified fluorine tin oxide electrodes, Analyst. 134 (2) (2009) 314–319, https://doi.org/10.1039/B809080G.